Available online at www.sciencedirect.com

ScienceDirect

Mendeleev Commun., 2020, **30**, 67–69

Mendeleev Communications

Photoinduced deprotonation of cyclopentene oxide radical cations in low-temperature Freon matrices

Ivan D. Sorokin,*[a] Oleg I. Gromov,[a] Vladimir I. Pergushov,[a] Daria A. Pomogailo[a,b] and Mikhail Ya. Melnikov[a]

[a] *Department of Chemistry, M. V. Lomonosov Moscow State University, 119991 Moscow, Russian Federation. E-mail: ivan.d.sorokin@gmail.com*

[b] *All-Russian Institute for Scientific and Technical Information, Russian Academy of Sciences, 125190 Moscow, Russian Federation*

DOI: 10.1016/j.mencom.2020.01.022

Upon the photolysis (λ = 546 nm) of X-ray irradiated cyclopentene oxide/Freon solutions at 77 K, irreversible proton abstraction in the ring-open form of the cyclopentene oxide radical cation occurs, affecting the bridgehead carbon. This affords unstable 6-oxabicyclo[3.1.0]hexan-1-yl radicals, which undergo rearrangement to form ring-open terminal C-centered alkyl radicals detected as final products.

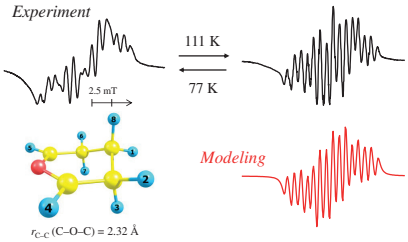

Keywords: photochemistry, intermediate, radical cation, EPR, UV/VIS, matrix, low temperature, cyclopentene oxide.

In recent years, interest in radical cations (RCs) has been refueled due to their prominence as intermediates in astrochemical transformations, biopolymer destruction, unusual electrochemical reactions, *etc*. However, these studies were devoted to the chemistry of RCs in their ground electronic states and, in select cases, upon their vibrational excitation, so-called hot RCs. These species were studied using quantum-chemical approaches and spectroscopic techniques including EPR and UV/VIS spectroscopy; however, the mechanistic aspects of the photochemical transformations of RCs remain poorly understood. The aim of our studies[–8] was to elucidate the photoinduced transformations of various RCs yielded by oxygen-, sulfur- and nitrogen-containing heterocyclic compounds using previous mechanistic interpretations for similar species.[·] The RCs of alkyl-substituted oxiranes were of particular interest as models because the direction and efficiency of processes occurring upon photoexcitation can be controlled by changing the number and nature of substituents at the oxirane ring.

Nevertheless, it is difficult to establish a clear relationship between the structure and the mechanisms and efficiencies of photoinduced transformations even for the methyloxirane RCs. No direct links to either spin density distribution or charge density distribution in the RCs could be established for the discovered mechanisms.[5–8] Specifically, the RC of cyclohexene oxide (CHO) was selected as a counterpart to the 2,3-dimethyloxirane RC, which underwent reversible photocyclization under the action of light.[5] However, instead of the expected slight differences in efficiencies, as compared to the 2,3-dimethyloxirane RC, the mechanism for the CHO RC in Freon matrices involved the transformation of the stabilized cyclic RC with an elongated C–C bond in the oxirane fragment along the pathway of photoinduced proton transfer to the matrix followed by thermally induced tunnel 1,2-transfer for the hydrogen atom with the resulting 7-oxabicyclo[4.1.0]heptan-2-yl radical as the final product[8]. This experimental result led us to investigate the related cyclopentene oxide (CPO) RC to determine the nature of its forms and ascertain whether conformational selection and the distribution of spin and charge density would affect the pathways and efficiencies of their photoinduced transformations.

We studied the transformations of RCs upon low-temperature matrix stabilization in Freon[†] matrices (commercial and synthesized using a published procedure). The experimental details were reported earlier.[5]

The quantum-chemical calculations were performed by the unrestricted density functional theory (DFT) method using the ORCA 4.1.1 program package. B2PLYP functional as well as the full-electron def2-TZVP basis set were used to calculate the geometry of potential energy surface (PES) minima. Geometries at minima were additionally checked for the presence of imaginary vibration frequencies. The spin-Hamiltonian parameters were calculated using the B3LYP functional together with the full-electron N07D basis set. The solvent effect was accounted for with the COSMO model.

The DFT calculations for stable RC geometries immediately revealed a major disparity between the yielded CPO and CHO RC. Interestingly, for the CPO RC, the cyclic form with a short C–C bond in the oxirane ring was unstable, as opposed to the CHO RC, where a form with a C–C bond length of 1.47 Å in the oxirane ring corresponded to a local PES minimum. The cyclic form of the CPO RC with an elongated C–C bond (1.7–1.8 Å) manifested itself in two PES local minima: the boat and chair conformations. For the chair conformation, the depth of the

[†] $CFCl_3$ (~99%, Aldrich), $CF_2ClCFCl_2$ (~99%, Aldrich) and CF_3CCl_3 (>99% based on NMR data, obtained from ~99% Aldrich $CF_2ClCFCl_2$) were used as matrices. Substrate CPO (~98%, Aldrich) was used without additional purification.

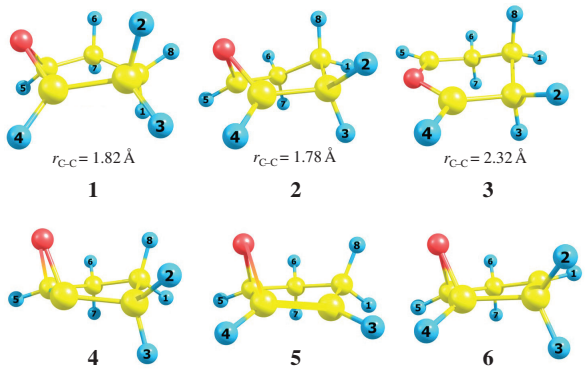

Figure 1 Calculated (DFT/B2PLYP/def2-TZVP) structures of the CPO-derived RCs (**1**–**3**) and corresponding radicals yielded upon deprotonation (**4**–**6**). The distances between two carbon atoms in the oxirane ring are given.

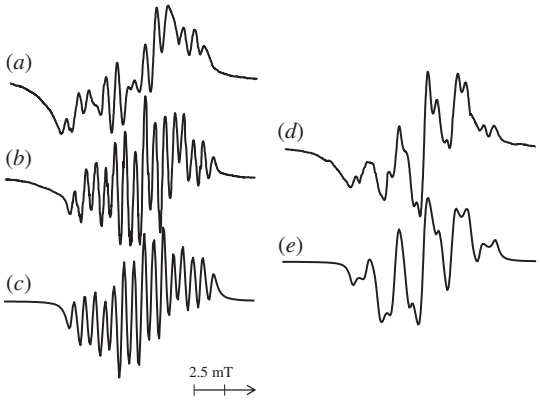

Figure 2 EPR spectra detected in irradiated CPO/CF_3CCl_3 solutions immediately upon (*a*) X-ray irradiation at 77 K and subsequent heating to 111 K [(*b*) experimental; (*c*) simulation with optimized parameters of form **3**, see Table 1], and upon the action of light with λ = 546 nm at 77 K [(*d*) experimental at 111 K; (*e*) spectrum simulated based on the calculated parameters of $^{\bullet}CH_2CH_2R$ radicals, see the text].

minimum was about 0.1 kJ mol^{-1}. The two forms were characterized by significant differences in their characteristic sets of hyperfine coupling (hfc) constants and, consequently, their EPR spectra (Figure 1, Table 1). Additionally, calculations of electron transitions for the described conformations using the complete active space self-consistent field method (CASSCF/NEVPT2/def2-QZVPP) revealed that the transitions of the ring-closed isomers lied in different regions of the visible absorption spectrum. Notably, the calculations predicted a significant red shift (>150 nm) for the major transition of the chair isomer (**1**, $\lambda_{max} \approx 615$ nm), as compared to the boat isomer (**2**, $\lambda_{max} \approx 465$ nm) and the ring-open isomer (**3**, $\lambda_{max} \approx 455$ nm) with a maximum distance (2.32 Å) between the carbon atoms of the oxirane ring. As expected, calculations showed that ring-open form **3** was the most stable in terms of energy (see Table 1).

Upon assessing the oscillator strength predictions for the major electronic transitions obtained *via* quantum-chemical calculations, we noted that the values for ring-open CPO RC form **3** ($f_{osc,\ 455} \approx 0.280$) and two cyclic CPO RC forms **1** ($f_{osc,\ 615} \approx 0.002$) and **2** ($f_{osc,\ 465} \approx 0.007$) differed by almost two orders of magnitude, precluding experimental detection of absorption bands for the chair (**1**) and boat (**2**) isomers. Initially, this unexpected result led us to believe that the photoinduced transformations described below could be associated with the possibility of RC photocyclization analogous to that observed earlier[7] for the RCs of methyloxiranes. However, further analysis of the detected EPR spectra proved that this interpretation would not be viable.

Upon X-ray irradiation of CPO/Freon solutions at 77 K, similar multiplet signals could be detected in the EPR spectra. Although the initial spectrum for the sample in CF_3CCl_3 [Figure 2(*a*)] differed slightly from those detected at 77 K in $CFCl_3$ and $CF_2ClCFCl_2$, the lines in the multiplet signal in CF_3CCl_3 could be resolved upon warming the samples to 111 K [Figure 2(*b*)]. Thus, the resulting spectrum closely resembled those in $CFCl_3$ and $CF_2ClCFCl_2$ at 77 K. The initial appearance of the spectrum was restored upon cooling the samples to 77 K. The experimental EPR spectra detected at 111 K could be successfully fitted using optimized parameters found in the calculations for form **3** of the RC [see Figure 2(*c*) and Table 1].

After the X-ray irradiation of samples in $CFCl_3$ and CF_3CCl_3 at 77 K with further photobleaching to remove the bands of matrix-derived intermediates, a broad absorption band appeared in a region of ~350–600 nm with a maximum at 490–500 nm in the UV/VIS spectra (Figure 3).

Upon the action of light with λ = 546 nm at 77 K on samples in the three Freon matrices, the absorption band at 490–500 nm perished irreversibly with a transformation in the EPR spectra. The multiplet spectrum attributed to CPO RC **3** gave way to a new five-line signal with additional splittings appearing in it upon sample heating from 77 to 111 K [Figure 2(*d*)]. Meanwhile, total integral intensity in the EPR spectrum was preserved. Therefore, the absorption band at 490–500 nm can be attributed to CPO RC **3**. No absorbance at 360–600 nm was detected in the UV/VIS spectra upon the action of light with λ = 546 nm. Consequently, the five-line signal in the EPR spectra can be attributed either to a distonic RC or to a carbon-centered radical formed upon deprotonation, as suggested earlier[8] for the CHO RC stabilized in Freon matrices. The calculated magnetic resonance parameters of all the distonic RCs formed upon intramolecular proton transfer cannot be used to attribute the experimental EPR spectra even qualitatively. Magnetic resonance parameters obtained by quantum-chemical calculations (see Figure 1, Table 2) for isomeric 6-oxabicyclo-[3.1.0]hexan-1-yl (**4**), 6-oxabicyclo[3.1.0]hexan-2-yl (**5**) or 6-oxabicyclo[3.1.0]hexan-3-yl (**6**) cannot be employed to generate

Table 1 DFT/B3LYP/N07D quantum-chemical calculation results for relative full energies, isotropic hfc constants with hydrogen nuclei (mT) and *g*-tensor components for the CPO-derived RCs and C-centered radicals that can be yielded by CPO RC upon proton transfer (based on geometries calculated by means of DFT/B2PLYP/def2-TZVP). Relative full energies are only given for the RCs. Fitting parameters of EPR spectra are given in parentheses.

RC	Magnetic resonance parameters								*g*-tensor components	*E*/kJ mol^{-1}
	$a_{iso}(H^1)$	$a_{iso}(H^2)$	$a_{iso}(H^3)$	$a_{iso}(H^4)$	$a_{iso}(H^5)$	$a_{iso}(H^6)$	$a_{iso}(H^7)$	$a_{iso}(H^8)$		
1	0.38	3.04	<0.10	1.25	1.25	3.05	<0.10	0.29	g_{xx} = 2.0072, g_{yy} = 2.0020, g_{zz} = 2.0047	126.3
2	<0.10	3.36	1.13	1.12	1.12	3.36	1.15	0.47	g_{xx} = 2.0077, g_{yy} = 2.0033, g_{zz} = 2.0047	105.9
3	0.13 (0.25)	0.83 (0.76)	3.19| (3.07)	1.72 (1.61)	1.73 (1.61)	0.82 (0.76)	3.18 (3.07)	0.16 (0.25)	g_{xx} = 2.0021, g_{yy} = 2.0022, g_{zz} = 2.0019	0
4	0.24	<0.10	0.10	-	0.20	0.22	<0.10	<0.10	g_{xx} = 2.0022, g_{yy} = 2.0033, g_{zz} = 2.0043	-
5	2.32	-	2.20	<0.10	0.13	<0.10	<0.10	4.15	g_{xx} = 2.0023, g_{yy} = 2.0030, g_{zz} = 2.0031	-
6	2.41	2.70	4.11	<0.10	<0.10	2.70	4.11	-	g_{xx} = 2.0024, g_{yy} = 2.0029, g_{zz} = 2.0030	-

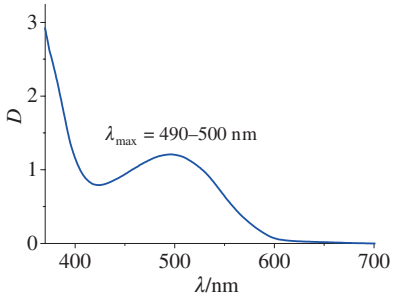

Figure 3 Difference UV/VIS spectrum detected in irradiated CPO/$CFCl_3$ solutions upon the action of light with λ = 546 nm at 77 K.

an EPR spectrum closely resembling the experimental EPR spectra [see Figure 2(*d*)]. Curiously, in our computations for radical **4**, we discovered that the calculated values for the hfc constants were very small owing to spin density localized in the vicinity of a strained three-membered ring. This is an unusual result for an alkyl radical of this type, which led us to believe that this species can rearrange into carbonyl-containing 2-oxocyclopentyl radicals. The calculated magnetic resonance parameters for 2-oxocyclopentyl radicals [a_1(1H) = 4.76 mT, a_2(1H) = 2.61 mT, a_3(1H) = 1.83 mT, a_4(1H) = 0.37 mT and a_5(1H) = 0.29 mT] and published data[18] can be used to generate a corresponding five-line EPR spectrum. Sadly, this did not lead to acceptable agreement between the shapes of lines in the fitted and experimentally observed spectra. There was another possible transformation pathway for radicals **4**: the formation of terminal alkyl $^{\bullet}CH_2CH_2R$ radicals. Their model EPR spectra [a_α(2H) ≈ 2.1 mT and a_β(2H) ≈ 2.4 mT] closely resembled the experimentally observed ones when the possible *g*-tensor anisotropy in the radicals was accounted for [$\Delta(g_{yy} - g_{xx}) \sim 0.007$; $\Delta(g_{yy} - g_{zz}) \sim 0.011$, Figure 2(*e*)]. Nevertheless, the ultimate interpretation of the structure of the C-centered radical formed upon the photolysis of the CPO RC may require additional research.

Molar absorption coefficients were calculated for the initial CPO RC absorption band arising upon radiolysis in $CFCl_3$ and CF_3CCl_3 by comparing changes in the absorbance and the number of paramagnetic centers determined in the EPR spectra. The values for the two Freons were quite close ($\varepsilon_{495} \approx 3.6\times10^3$ $dm^3cm^{-1}mol^{-1}$) and consistent with those found for ring-open forms of RCs derived from methyloxiranes.[7] The quantum yields ($\varphi_{546} \approx 0.003$ in CF_3CCl_3 and $\varphi_{546} \approx 0.01$ in $CFCl_3$) measured at the initial stage of CPO RC photolysis (Scheme 1) were noticeably lower than those found in the photoinduced transformations of CHO RC ($\varphi_{546} \approx 0.02$ in CF_3CCl_3 and $\varphi_{546} \approx 0.06$ in $CFCl_3$).

Thus, we can conclude that irreversible proton abstraction from the bridgehead carbon in ring-open RC **3** most likely occurs upon the photolysis of X-ray-irradiated CPO/Freon solutions (where RC **3** is the primary radiolysis product) at 77 K (λ = 546 nm). Unstable 6-oxabicyclo[3.1.0]hexan-1-yl radicals **4** rearrange to form C-centered terminal alkyl radicals, which were detected as final products in the Freon matrices. Apparently, different stabilities of CHO and CPO-derived neutral radicals result in different final photolysis products for each of the radical cationic species (even though the general photolysis mechanism is similar in both cases). Interestingly, the proton transfer photolysis mechanism that manifests itself in the CHO and CPO RCs is not common for oxirane RCs with non-cyclic substituents at the oxirane ring. This can be due to steric hindrances in the bulkier CHO and CPO RCs.

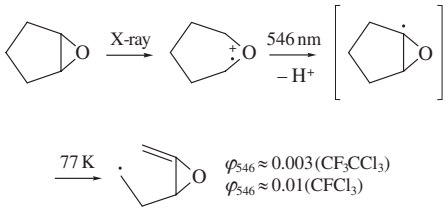

Scheme 1

This work was supported by the Russian Foundation for Basic Research (project no. 19-03-00015) with the use of equipment purchased on behalf of the Development Program of Moscow State University. Calculations were performed using the resources of the Supercomputing Center of M. V. Lomonosov Moscow State University.

References

1 V. I. Feldman, S. V. Ryazantsev, E. V. Saenko, S. V. Kameneva and E. S. Shiryaeva, *Radiat. Phys. Chem.*, 2016, **124**, 7.
2 A. Banyasz, T.-M. Ketola, A. Muñoz-Losa, S. Rishi, A. Adhikary, M. D. Sevilla, L. Martinez-Fernandez, R. Improta and D. Markovitsi, *J. Phys. Chem. Lett.*, 2016, **7**, 3949.
3 E. J. Horn, B. R. Rosen and P. S. Baran, *ACS Cent. Sci.*, 2016, **2**, 302.
4 E. A. Solano and P. M. Mayer, *J. Chem. Phys.*, 2015, **143**, 104305.
5 I. D. Sorokin, V. I. Feldman, O. L. Mel'nikova, V. I. Pergushov, D. A. Tyurin and M. Ya. Mel'nikov, *Mendeleev Commun.*, 2011, **21**, 153.
6 I. D. Sorokin, V. I. Feldman, O. L. Mel'nikova, V. I. Pergushov, D. A. Tyurin and M. Ya. Mel'nikov, *Mendeleev Commun.*, 2011, **21**, 155.
7 I. D. Sorokin, O. L. Melnikova, V. I. Pergushov, D. A. Tyurin, V. I. Feldman and M. Ya. Melnikov, *High Energy Chem.*, 2012, **46**, 183 (*Khim. Vys. Energ.*, 2012, **46**, 228).
8 I. D. Sorokin, O. I. Gromov, V. I. Pergushov, D. A. Pomogailo and M. Ya. Mel'nikov, *Mendeleev Commun.*, 2018, **28**, 618.
9 K. Ushida, T. Shida and K. Shimokoshi, *J. Phys. Chem.*, 1989, **93**, 5388.
10 M. Lindgren and M. Shiotani, in *Radical Ionic Systems. Properties in Condensed Phases. ESR Studies of Radical Cations of Cycloalkanes and Saturated Heterocycles*, eds. A. Lund and M. Shiotani, Kluwer Academic, Dordrecht, 1991, vol. 6, pp. 125–150.
11 W. T. Miller, E. W. Fager and P. H. Griswald, *J. Am. Chem. Soc.*, 1950, **72**, 705.
12 F. Neese, *Wiley Interdiscip. Rev.: Comput. Mol. Sci.*, 2018, **8**, e1327.
13 S. Grimme, *J. Chem. Phys.*, 2006, **124**, 034108.
14 F. Weigend and R. Ahlrichs, *Phys. Chem. Chem. Phys.*, 2005, **7**, 3297.
15 V. Barone, P. Cimino and E. Stendardo, *J. Chem. Theory Comput.*, 2008, **4**, 751.
16 S. Sinnecker, A. Rajendran, A. Klamt, M. Diedenhofen and F. Neese, *J. Phys. Chem. A*, 2006, **110**, 2235.
17 M. Ya. Melnikov, D. V. Baskakov and V. I. Feldman, *High Energy Chem.*, 2002, **36**, 309 (*Khim. Vys. Energ.*, 2002, **36**, 346).
18 P. Smith, C. I. Weathers and W. H. Donovan, *J. Magn. Reson.*, 1988, **79**, 124.
19 I. D. Sorokin, V. I. Pergushov, L. I. Savostina and M. Ya. Melnikov, *High Energy Chem.*, 2014, **48**, 180 (*Khim. Vys. Energ.*, 2014, **48**, 219).
20 V. Sadovnichy, A. Tikhonravov, Vl. Voevodin and V. Opanasenko, in *Contemporary High Performance Computing: From Petascale toward Exascale*, ed. J. S. Vetter, CRC Press, Boca Raton, 2013, pp. 283–307.

Received: 25th June 2019; Com. 19/5965